Received: 7 November 2019 | Revised: 18 December 2019 | Accepted: 6 January 2020

DOI: 10.1002/btpr.2958

RESEARCH ARTICLE

Formulation and Engineering of Biomaterials

BIOTECHNOLOGY PROGRESS

Next-generation polymerized human hemoglobins in hepatic bioreactor simulations

Clayton Cuddington[1] | Savannah Moses[1] | Donald Belcher[1] | Niral Ramesh[2] | Andre Palmer[1]

[1]Department of Chemical and Biomolecular Engineering, The Ohio State University, Columbus, Ohio

[2]Department of Chemical and Biomolecular Engineering, Rice University, Houston, Texas

Correspondence
Andre Palmer, Department of Chemical and Biomolecular Engineering, The Ohio State University, 151 W. Woodruff Ave., Columbus, OH 43210.
Email: palmer.351@osu.edu

Funding information
National Institutes of Health, Grant/Award Numbers: R01EB021926, R01HL126945, R01HL138116; U.S. Department of Defense, Grant/Award Number: W81XWH-18-1-0059

Peer Review
The peer review history for this article is available at https://publons.com/publon/10.1002/btpr.2958.

Abstract

Hepatic hollow fiber (HF) bioreactors can be used to provide temporary support to patients experiencing liver failure. Before being connected to the patient's circulation, cells in the bioreactor must be exposed to a range of physiological O_2 concentrations as observed in the liver sinusoid to ensure proper performance. This zonation in cellular oxygenation promotes differences in hepatocyte phenotype and may better approximate the performance of a real liver within the bioreactor. Polymerized human hemoglobin (PolyhHb) locked in the tense quaternary state (T-state) has the potential to both supply and regulate O_2 transport to cultured hepatocytes in the bioreactor due to its low O_2 affinity. In this study, T-state PolyhHb production and purification processes were optimized to minimize the concentration of low-molecular-weight PolyhHb species in solution. Deconvolution of size-exclusion chromatography spectra was performed to calculate the distribution of polymeric Hb species in the final product. Fluid flow and mass transport within a single fiber of a hepatic HF bioreactor was computationally modeled with finite element methods to simulate the effects of employing T-state PolyhHb to facilitate O_2 transport in a hepatic bioreactor system. Optimal bioreactor performance was defined as having a combined hypoxic and hyperoxic volume fraction in the extracapillary space of less than 0.05 where multiple zones were observed. The Damköhler number and Sherwood number had strong inverse relationships at each cell density and fiber thickness combination. These results suggest that targeting a specific Damköhler number may be beneficial for optimal hepatic HF bioreactor operation.

KEYWORDS

fluid flow modeling, hemoglobin-based oxygen carrier, hollow fiber bioreactor, polymerized human hemoglobin, red blood cell substitute

1 | INTRODUCTION

Hepatic hollow fiber (HF) bioreactors have the potential to support patients who are suffering from acute liver failure.[1] Cell culture media used to provide nutrients to hepatocytes in HF bioreactors must be supplemented with an oxygen (O_2) carrier in order to provide O_2 offloading ability. To date, there is no practical O_2 carrier for use in HF bioreactors such as those employed as a bioartificial liver assist devices.[2] Because red blood cells (RBCs) undergo hemolysis in these devices, blood is an ineffective choice for use as an O_2 carrier in the perfusate.[3] Therefore, the goal of this work is to create a perfusate that can adequately oxygenate the high cell density found in the extracapillary space (ECS) of HF bioreactors. Given that hemoglobin (Hb) is the natural O_2 transport molecule in vivo,[4] Hb is a potential choice for improving O_2 transport in an HF bioreactor. However, the small size of Hb [molecular weight (MW) of 64 kDa and an effective diameter of 5 nm] limits its application in a perfusate solution.[5] This free protein, as well as other low MW Hb species (<500 kDa), are small enough to extravasate through the membrane in the HF bioreactor. After extravasating into the ECS, Hb can come in to direct contact with cells residing in the ECS. When in direct contact with the cells in the ECS, the reactive O_2 species generated by unmodified Hb result in oxidative tissue damage and cell death.[6,7]

To prevent these harmful effects, Hb can be modified to create an Hb-based O_2 carrier (HBOC).[8,9] HBOCs are a promising class of RBC substitute. Popular forms of Hb modification include PEGylation, surface conjugation, encapsulation, and polymerization.[10,11] Of these, polymerized Hb (PolyHb) is the most viable due to its low cost and scalability.[11] Polymerization of Hb with glutaraldehyde as a nonspecific crosslinker is a common strategy used in the synthesis of previous generations of PolyHbs.[12] However, these earlier generation PolyHbs were not effective because they contained large amounts of free Hb and other low MW polymeric Hb species.[13-15]

Previous studies have shown that the average size of PolyHb can be altered by varying the molar ratio of glutaraldehyde to Hb. While this modification increases the average MW of PolyHb, it does not eliminate the presence of low MW polymeric Hb species.[16,17] To address this issue, a two-stage tangential flow filtration (TFF) system can be employed.[18,19] The product is first passed through a 0.2 μm TFF filter cartridge to remove large PolyHb aggregates. It is then diafiltered over a TFF filter cartridge with MW cutoff on the order of hundreds of kDa to remove as much low MW PolyHb as possible. The final PolyHb product would then have a viable MW distribution for use in bioreactor or ex vivo organ circuits.

The primary drawback of hepatic HF bioreactors is insufficient O_2 transport to support a high density of hepatocytes in the ECS.[20,21] Ideally, O_2 transport across the membrane would be regulated to mirror the hepatic O_2 gradient observed in vivo. Prior research has demonstrated that polymerized human Hb (PolyhHb) frozen in the tense quaternary state (T-state) can regulate O_2 transport to cells housed in the ECS.[17] This can prevent the development of hypoxia and hyperoxia, allowing the hepatocytes to function more effectively. Additionally, hepatic cells must be exposed to a range of physiological O_2 concentrations as observed in the liver sinusoid, which is known as zonation, to properly function.[1,22]

This study builds on previous work and explores a method of quantifying zonation as well as general bioreactor performance. The HF length, single capillary system radius, perfusate flow rate, inlet O_2 partial pressure ($pO_{2,in}$), HBOC concentration, and cell density were varied to determine their effect on bioreactor operation. Two dimensionless numbers, the Damköhler number and Sherwood number, were calculated within the bioreactor system, and their relationship to overall bioreactor performance and zonation was evaluated. The primary objective was to determine which variables and dimensionless numbers strongly correlate to bioreactor performance and zonation.

2 | MATERIALS AND METHODS

2.1 | Materials

Glutaraldehyde (70%), sodium chloride (NaCl), potassium chloride (KCl), sodium hydroxide (NaOH), sodium dithionite ($Na_2S_2O_4$), calcium chloride ($CaCl_2{\cdot}2H_2O$), sodium lactate, *N*-acetyl-L-cysteine (NALC), sodium cyanoborohydride ($NaCNBH_3$), sodium phosphate dibasic (Na_2HPO_4), and sodium phosphate monobasic (NaH_2PO_4) were purchased from Sigma-Aldrich (St. Louis, MO). HF TFF modules (PES 0.2 μm and PS 500 kDa) were purchased from Spectrum Laboratories (Rancho Dominguez, CA). All other chemicals were purchased from Fisher Scientific (Pittsburgh, PA). Expired human RBC units were generously donated by Transfusion Services, Wexner Medical Center, The Ohio State University, Columbus, OH.

2.2 | PolyhHb synthesis

Human hemoglobin (hHb) was first purified via TFF as described by Palmer et al.[23] Glutaraldehyde was used as the crosslinking agent at a 30:1 molar ratio of glutaraldehyde to hHb as described previously.[24,25]

The hHb was diluted to 40 ± 5 g/L in phosphate-buffered saline (PBS) (0.1 M, pH 7.4) and filtered through a 0.2 μm polysulfone (PS) TFF module to remove any large aggregates formed during cryogenic storage.

The hHb was further diluted with PBS to a total working volume of 1,500 ml at a concentration of 19.5 ± 1 g/L. The solution was then added to an airtight glass reaction vessel. The solution was mixed continuously with a stir bar and constant temperature was maintained by placing the reaction vessel in a water bath at 37°C. The hHb solution was deoxygenated via continuous recirculation through a 3M MiniModule gas exchange membrane (Maplewood, MN). The solution partial pressure of dissolved O_2 (pO_2) was verified on a Rapidlab 248 (Siemens, Malvern, PA) blood gas analyzer (BGA). Once the pO_2 was below 10 mmHg, $Na_2S_2O_4$ was used to remove the remaining O_2 dissolved in solution. An initial bolus addition of 300 mg was dissolved in 50 ml PBS sparged with

nitrogen (N_2), followed by four 50 mg additions in 1 ml deoxygenated PBS over 15 min intervals. A final BGA reading was taken to ensure the pO_2 was below detectable levels (<0 mmHg).

A 30:1 molar ratio of glutaraldehyde to hHb was then added to the reactor at 2 ml/min using a syringe pump (New Era Pump Systems, Farmingdale, NY). After the glutaraldehyde addition was completed, the solution was allowed to polymerize for 2 hr under positive N_2 pressure in the reactor headspace.

The polymerization reaction was then quenched at ambient temperature (20°C) with a 7:1 molar ratio $NaCNBH_3$ to glutaraldehyde. The addition of $NaCNBH_3$ also reduces the Schiff bases in solution and minimizes methemoglobin (metHb) levels in the final product. The PolyhHb solution was quenched at ambient temperature for 30 min and then the vessel was stored at 4°C overnight.

2.3 | PolyhHb purification and diafiltration

All purification steps took place in a 4°C refrigerator. The PolyhHb solution was first passed through a 0.2 μm PS TFF cartridge to remove large polymeric Hb species from the solution. Diafiltration over a 500 kDa TFF cartridge then removed low MW polymeric Hb species, unpolymerized hHb, and unreacted glutaraldehyde. The difiltration occurs simultaneously with an excipient exchange with modified Ringer's lactate (NaCl 115 mmol/L, KCl 4 mmol/L, $CaCl_2{\cdot}2H_2O$ 1.4 mmol/L, NaOH 13 mmol/L, NALC 12.3 mmol/L, and sodium lactate 27 mmol/L) at pH 7.4. After 10× volume exchanges, the hHb concentration of the permeate of the 500 kDa TFF cartridge was measured using a UV–vis spectrometer (Olis Inc., Bogart, GA) to validate that the free hHb concentration was less than 1 mg/ml.[26] The PolyhHb solution was concentrated to a final PolyhHb concentration greater than 10 g/dL. The cyanomethemoglobin method was used to measure the metHb level and final concentration of the PolyhHb solution.[27] The final product was stored at −80°C. All tubing and equipment was sterilized using 0.1 M NaOH.

2.4 | Oxygen equilibrium measurements

O_2 equilibrium curves (OEC) for hHb and PolyhHb were measured using a Hemox Analyzer (TCS Scientific Corp., New Hope, PA) at 37°C (physiological temperature). The O_2 binding data from these experiments were fit to the Hill equation to regress the resultant partial pressure of O_2 at which 50% of the hHb or PolyhHb is saturated with O_2 (P_{50}) and cooperativity coefficient (n).[28]

2.5 | Size-exclusion chromatography

High-performance liquid chromatography (HPLC) coupled with size-exclusion chromatography (SEC) was performed with an Ultimate 3000 system using an SEC-1000 column (ThermoFisher Scientific, Waltham, MA). The absorbance was measured at 412 nm to monitor the Soret peak of Hb in the sample. The resultant intensity versus time data was scaled such that the maximum intensity for each run was set to 1. These data were then used to determine the size and MW of the PolyhHbs.

2.5.1 | Spectral deconvolution

SEC data were analyzed using a novel computational program in RStudio (Version 1.1.456, RStudio, Inc., Boston, MA). PolyhHbs of different sizes were characterized by their "polymer order" (n_o), which corresponds to how many times the Hb polymer doubled in size to reach its current mass. This was defined as

$$N_{Hb} = 2^{n_o}, \quad (1)$$

where N_{Hb} is the number of hHb tetramers in the Hb polymer.

Since the MW of a single hHb tetramer is 64 kDa, Equation (1) was scaled to

$$MW_{Polymer}(kDa) = 64 \times 2^{n_o}, \quad (2)$$

such that a zeroth-order polymer (unpolymerized hHb) corresponds to 1 hHb tetramer in Equation (1) and 64 kDa in Equation (2).

The SEC elution time was calibrated to hHb according to the equation

$$MW(Da) = 10^{-0.7339 \times \text{elution time} + 11.855}. \quad (3)$$

Equations (2) and (3) were combined to determine the elution times of the various polymer orders. Gaussian curves at each polymer order elution time were scaled to fit the total elution curve of the PolyhHb mixture. The scaled normal curves of the polymeric Hb species were used to calculate the fraction of each polymer order in the final PolyhHb product.

2.6 | Auto-oxidation

A representative sample of 30:1 T-state PolyhHb was removed from cryogenic storage and allowed to thaw. The sample was then diluted to 12.5 mg/ml, which corresponds to a typical HBOC concentration in the circulation immediately after transfusion as well as the primary PolyhHb concentration in the bioreactor simulations.[29,30] The 630 nm peak of the sample was monitored over 24 hr by UV–vis spectrometry. The cuvette was kept at 37°C to replicate physiological conditions. The same protocol was repeated for hHb as a control for metHb levels over time.

2.7 | Model hepatic HF bioreactor

For this model, we computationally examined a single fiber of a hepatic HF bioreactor utilizing T-state PolyhHb as the O_2 carrier, which is shown in Figure 1. Both fluid flow and O_2 mass transport

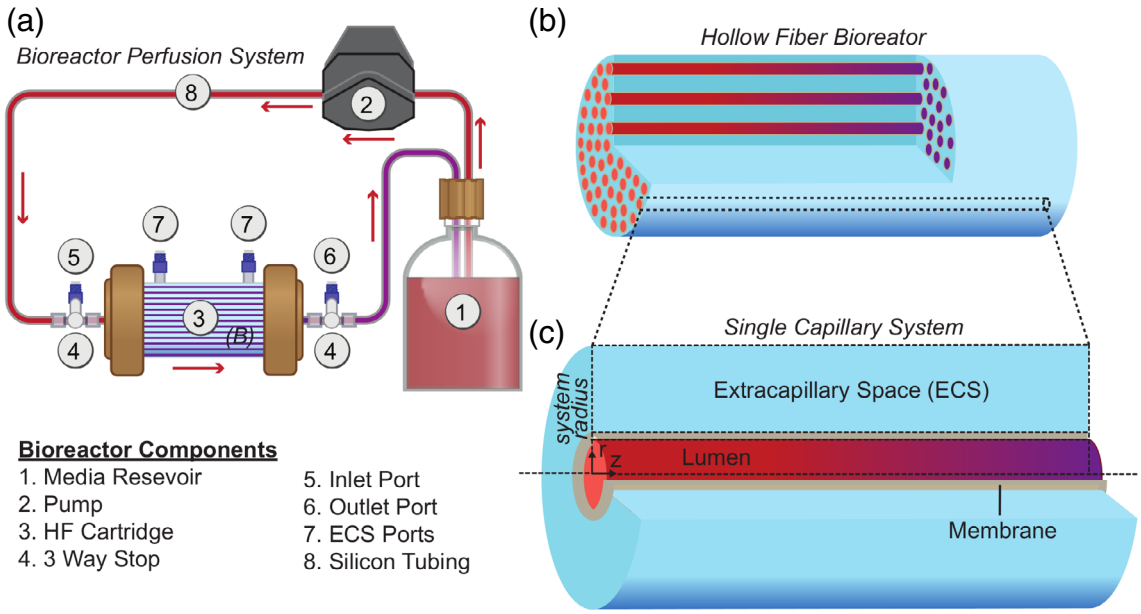

FIGURE 1 Diagram of the (a) entire bioreactor circuit (b) internal structure of the HF bioreactor, and (c) geometry of a singular fiber and surrounding extracapillary space (ECS)

with reactions were computationally modeled using finite element methods in COMSOL Multiphysics version 5.3a (COMSOL Inc., Burlington MA). The model physics are unchanged from a recent publication.[17] The HF radius, fiber length, flow rate, inlet O_2 concentration, cell density, and PolyhHb concentration were each varied to evaluate preferred bioreactor operating conditions.

2.8 | Dimensionless numbers

To assess PolyhHb-mediated mass transfer of O_2 from the HF lumen into the ECS, we examined the Sherwood number, also known as the mass-transfer Nusselt number, which is calculated as shown below.

$$\mathrm{Sh} = k_c \frac{2R_{\mathrm{lumen}}}{D_{O_2}}, \tag{4}$$

where R_{lumen} is the outer radius of the lumen, D_{O_2} is the diffusivity of O_2 in the lumen, and k_c is the mass transfer coefficient, which was calculated as follows:

$$k_c = \frac{J_{O_2}}{[O_2]_{\mathrm{lumen}} - [O_2]_{\mathrm{ECS}}}. \tag{5}$$

To relate how the O_2 consumption rate (OCR) by the cells in the ECS compared to the residence time in the system, we used a theoretical form of the Damköhler number [Damkohler number $(\mathrm{Da})_{\mathrm{theor}}$] as shown below.

$$\mathrm{Da}_{\mathrm{theor}} = \tau \frac{\mathrm{OCR}}{[O_2]_{\mathrm{ECS}}}, \tag{6}$$

where $[O_2]_{\mathrm{ECS}}$ is the concentration of O_2 in the ECS, and the residence time is defined as follows:

$$\text{Residence time} = \tau = \frac{V_{\mathrm{ECS}}}{Q_{\mathrm{in}}}, \tag{7}$$

where V_{ECS} is the volume of the ECS and Q_{in} is the total volumetric flow rate of PolyhHb supplemented media in the system. The OCR of cells in the ECS is calculated by evaluating the net concentration of O_2 entering the HF (accounting for both dissolved O_2 and Hb bound O_2) divided by the residence time.

$$\mathrm{OCR} = \frac{[\mathrm{HbO_2}]_{\mathrm{in}} - [\mathrm{HbO_2}]_{\mathrm{out}} + [O_2]_{\mathrm{in}} - [O_2]_{\mathrm{out}}}{\tau}. \tag{8}$$

Unfortunately, the theoretical Damköhler number uses the average ECS O_2 concentration, which is difficult to measure within the bulk of large HF modules that can contain bundles of more than 1,000 fibers. Because of this limitation, we also define a practical Damköhler ($\mathrm{Da}_{\mathrm{pract}}$) number that uses the average of the inlet and outlet O_2 concentrations as an approximation. Since the latter is more straightforward to measure during the experimental operation of the bioreactor, it is primarily presented in our analysis.

$$\mathrm{Da}_{\mathrm{pract}} = \frac{2\tau \cdot \mathrm{OCR}}{[O_2]_{\mathrm{in}} + [O_2]_{\mathrm{out}}}. \tag{9}$$

2.9 | Zonation

The bioreactor volume is divided into five zones based on the pO_2 present. The thresholds for each zone are given below:

$$\text{Hypoxic (H)} = pO_2 < 20\,\text{mmHg},$$

$$\text{Perivenous (Pv)} = 20\,\text{mmHg} < pO_2 < 35\,\text{mmHg},$$

$$\text{Pericentral (Pc)} = 35\,\text{mmHg} < pO_2 < 60\,\text{mmHg},$$

$$\text{Periportal (Pp)} = 60\,\text{mmHg} < pO_2 < 70\,\text{mmHg},$$

$$\text{Hyperoxic (Hr)} = pO_2 > 70\,\text{mmHg}.$$

For these simulations, we considered situations where the zonation was balanced between the perivenous, pericentral, and periportal regions. To quantify when this kind of zonation occurred, we calculated a zonation score (Z) by dividing the average absolute deviation of the perivenous, pericentral, and periportal volume fractions divided by the sum of the perivenous, pericentral, and periportal volume fraction.

$$Z = \frac{\sum_{i}^{n_f} | V_{f,i} - n_f^{-1} \cdot \sum_{i}^{n_f} V_{f,i} |}{n_f \cdot \sum_{i}^{n_f} V_{f,i}}, \quad (10)$$

where $V_{f,\,i}$ is the volume of the ith zone, and n_f is the total number of zones considered. For our model, we only considered pericentral, perivenous, and periportal regions so n_f was set to 3.

3 | RESULTS AND DISCUSSION

There are multiple biophysical metrics to assess the efficacy of PolyhHb as an HBOC. Table 1 shows the concentration (C), metHb level, hydrodynamic diameter of PolyhHb (D_{PolyhHb}), MW, P_{50}, n, and rate constant of auto-oxidation (k_{ox}) for both 30:1 T-state PolyhHb and unmodified hHb.

3.1 | Protein concentrations

The 30:1 T-state PolyhHb produced was concentrated to 10.1 ± 0.6 g/dl. This concentration is comparable to previous commercial HBOCs: PolyHeme 10 g/dl[31] and Hemolink 9.7 g/dl.[32]

TABLE 1 Biophysical properties for unmodified hHb compared to 30:1 T-state PolyhHb

Species	hHb	30:1 T-state PolyhHb
C (g/dl)	21 ± 5	10.1 ± 0.6
metHb (%)	2.0 ± 0.6	5.7 ± 1.6
D_{PolyhHb} (nm)	5.5 34	45 ± 6
MW (kDa)	64 ± 2	1,300 ± 100
P_{50} (mmHg)	12.8 ± 0.1	41 ± 3
n	2.9 ± 0.1	1.0 ± 0.1
k_{ox} (h^{-1})	0.0432 ± 0.001	0.0261 ± 0.006

The metHb level of the final PolyhHb was more than double that of unmodified hHb. This can be explained by two different steps in the synthesis procedure. During polymerization, hHb in the reactor was maintained at 37°C for approximately 2 hr. While the reaction was eventually quenched with $NaCNBH_3$, which reduces metHb in solution, there was still an increase in the metHb level at this step. Additionally, previous studies have shown that there is auto-oxidation that occurs during TFF purification leading to further increases in the metHb level.[19,33] Decreasing the temperature during TFF can lead to less metHb formation, so the solution temperature during TFF was reduced from 4°C to approximately 0°C by submerging the purification vessels in ice. The resultant metHb levels fell from 6.76 ± 1.3% to 4.69 ± 1.1% confirming that TFF processing increases metHb levels above that of unmodified hHb. The metHb levels were similar between 30:1 T-state PolyhHb and commercial HBOCs. The biophysical properties of some previous generation HBOCs are shown in Table 2.

3.2 | Hydrodynamic diameter of PolyhHb

The D_{PolyhHb} of 30:1 T-state PolyhHb (45 ± 11 nm) is significantly larger ($p < .05$) than the reported diameter of free Hb, 5.5 nm.[34] The increased diameter of PolyhHb will help mitigate the negative side effects associated with free Hb in a bioreactor such as free heme release, extravasation to the cells in the ECS, and oxidative tissue damage.[35]

3.3 | Oxygen equilibrium

The O_2-Hb binding data were fit to the Hill equation. The resulting data and fit are shown in Figure 2. From this fit, the P_{50} and n were determined. The differences between the P_{50} and cooperativity in hHb and PolyhHb are shown to be statistically significant. The 30:1 T-state O_2-PolyhHb binding curve is not sigmoidal, unlike the O_2-Hb binding curve. The absence of sigmoidal O_2 binding represents a loss of cooperativity after Hb is cross-linked. Cooperativity is a function of the quaternary structure of the Hb protein. After being locked in the T-state, the quaternary structure is unable to change, and consequently, cooperativity is lost in PolyhHbs.[36]

The other notable change that results from polymerizing deoxygenated Hb is the right shift in the P_{50}. Polymerization restricts the resultant PolyhHb to the T-state conformation.[37] The right shift in the OEC corresponds to a lower O_2 affinity and a greater O_2 offloading ability. This increased O_2 offloading potential is vital for optimal bioreactor function as it allows oxygenation across physiologically relevant O_2 tensions. The P_{50} of T-state PolyhHb is comparable to the P_{50} of Oxyglobin, Hemopure (Biopure Corp., Cambridge, MA), and Hemolink (Hemosol Inc., Toronto, Canada), yet is notably larger than that of PolyHeme (Northfield Laboratories Inc., Northfield, IL). The cooperativity coefficient is comparable to that of Hemolink but is lower than other commercial HBOCs. The increased cooperativity of previous HBOCs likely results from the large amounts of tetrameric Hb present in most commercial HBOCs.

TABLE 2 Biophysical parameter comparison of 30:1 T-state PolyhHb to commercial HBOCs

HBOC	Avg. MW (kDa)	P_{50} (mmHg)	*n*	metHb (%)	% <500 kDa
Oxyglobin	200 38	38 44	1.4 44	5.08 45	100
Hemopure (HBOC-201)	250 38	37 38	1.4 31	<10 31	78 ± 1.1
Hemolink	190 18	39 38	0.95 32	6.55 32	66.2 ± 0.2
PolyHeme	150 38	29 38	1.7 31	<8 31	Not tested
30:1 T-state PolyhHb	1,300 ± 100	41 ± 3	1.0 ± 0.1	5.7 ± 1.6	4.6 ± 1.6

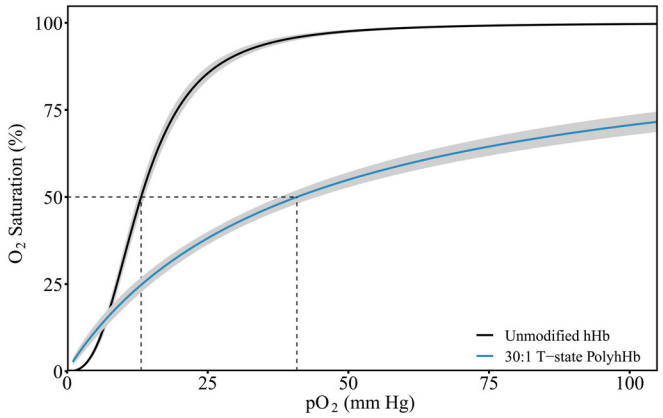

FIGURE 2 O_2 equilibrium curves for 30:1 T-state PolyhHb compared to unmodified hHb with their respective standard deviations shown in gray. Measured at 37°C in pH 7.4 Hemox buffer

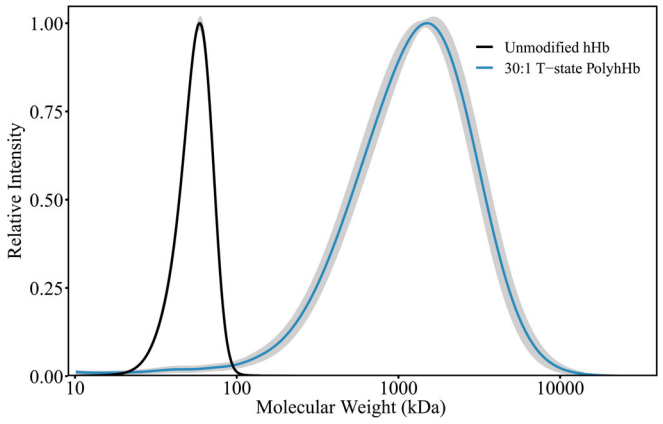

FIGURE 3 Average molecular weight (MW) distributions for 30:1 T-state PolyhHb and unmodified hHb with their respective standard deviations displayed in gray. MW was calculated by transforming the time axis of the size-exclusion chromatography (SEC) plot to the corresponding MW using a calibration curve

3.4 | Size-exclusion chromatography

The average SEC curve of 16 PolyhHb batches is shown in Figure 3. The PolyhHb displays a relatively Gaussian size distribution, indicating uniform MW dispersion. This is further demonstrated by the narrow standard deviation around the average SEC curve. For comparison, the average curve for unmodified hHb is also shown in Figure 3. There is minimal overlap between the hHb curve and the PolyhHb curve demonstrating that the final PolyhHb product contains nearly zero hHb. The primary difference between commercial HBOCs and the one synthesized in this study is their size as determined by MW. Previous PolyhHbs such as Hemopure and PolyHeme contain more than 10% unmodified hHb,[31,38] which has been shown to cause cell toxicity for hepatocytes.[39,40] PolyhHbs from this study have an average MW that is five to eight times larger than that of previous commercial HBOCs.

3.4.1 | Spectral deconvolution

Equations (1), (2), and (3) yield Table 3 when calculations are taken out to the fifth polymer order. In this study, sixth-order and larger polymers are not present in the final PolyhHb product as they are retained on the 0.2 μm TFF module during the PolyhHb purification process.

The deconvolution plot of the average PolyhHb SEC curve is shown in Figure 4 to provide a visual representation of how the SEC deconvolution function fits the various polymer order normal curves to the total SEC data. As is evident both visually by the fit as well as the R-squared value, 0.99996, curve fitting the Hb polymer orders describes the overall HPLC-SEC curve very well.

This deconvolution process was applied to all PolyhHbs synthesized in this study. The results are shown in Figure 5. It should be noted that only 4.6% of the average PolyhHb synthesized was comprised of polymeric Hb species less than 500 kDa, which has traditionally been the highest MW reported for previous generation HBOCs.[18,38] As discussed previously, this reduction in low MW Hb species should mitigate many of the negative side effects associated with prior HBOCs.

3.5 | Auto-oxidation

Prior literature has demonstrated that Hb oxidizes in a first-order manner.[41,42] Using this information, the ferrous Hb concentration as a function of time was linearized by taking the natural logarithm of concentration as shown in Figure 6. k_{ox}, of unmodified Hb agreed with the value previously reported by Meng et al.[43] The auto-oxidation rate for 30:1 T-state PolyhHb was less than half of that for Hb. This results from the size difference of PolyhHb compared to Hb. The

TABLE 3 Breakdown of the makeup and properties of the six polymer orders observed in 30:1 T-state PolyhHb

	Zeroth-order	First-order	Second-order	Third-order	Fourth-order	Fifth-order
Number of Hb tetramers	1	2	4	8	16	32
Elution time (min)	9.6046	9.1944	8.7842	8.3741	7.9639	7.5537
MW (kDa)	64	128	256	512	1,028	2,048

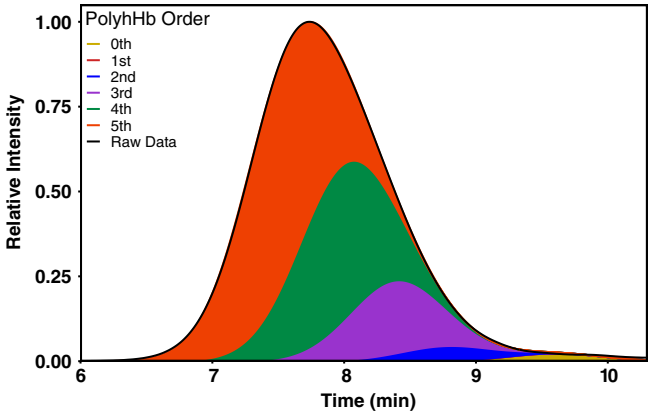

FIGURE 4 Hb polymer order normal curves scaled and summed to fit the raw size-exclusion chromatography (SEC) data for the average 30:1 T-state PolyhHb curve

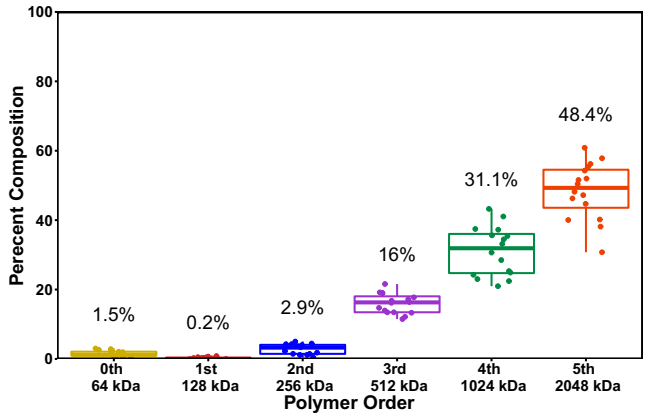

FIGURE 5 Hb polymer order composition of each PolyhHb shown as percent total of the final product

larger size of 30:1 T-state PolyhHb creates more steric hindrance for O_2 to bind to the heme pocket. This shielding effect may prevent oxidation from happening as quickly compared to hHb. Additionally, the 30:1 T-state PolyhHb was stored in modified Ringer's lactate, which contains NALC. NALC is a reducing agent that was specifically added to the solution to prevent Hb oxidation. While the test samples were diluted in PBS, there was still residual Ringer's lactate present in solution to slow metHb formation.

The lower auto-oxidation rate constant of 30:1 T-state PolyhHb compared to unmodified Hb indicates it may be suitable for extended use in an HF bioreactor. By maintaining the heme iron in the ferrous state, it will be able to bind and release O_2 as intended for a sustained

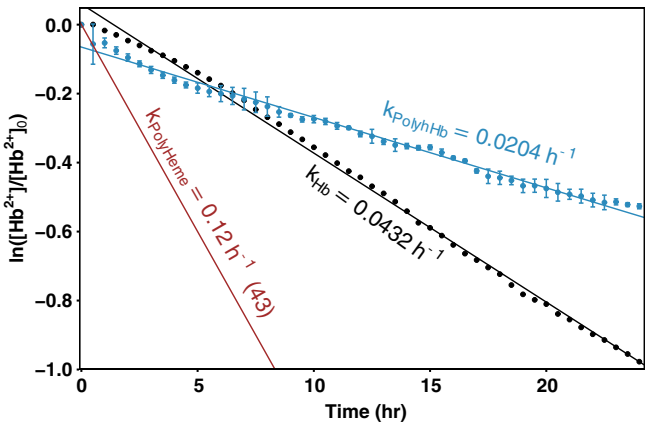

FIGURE 6 Auto-oxidation first-order kinetics linearized plots for unmodified hHb and 30:1 T-state PolyhHb with standard deviations. Tests were performed at 37°C in pH 7.4 phosphate-buffered saline (PBS) over a 24 hr time course using a UV–visible spectrometer

period of time. With a lower k_{ox} value, the PolyhHb perfusate will remain functional for a longer duration in the perfusion circuit. This will maintain the intended O_2 gradient across the HF hepatic bioreactor for a longer duration and will require fewer replacements of the perfusion solution.

3.6 | Simulated bioreactor

The effect of cell density on the combined hypoxic and hyperoxic fraction at various single capillary system radii, PolyhHb concentrations, and $pO_{2,in}$ values is shown in Figure 7. At all system radii, there is an optimal point with minimized hypoxic and hyperoxic conditions. Decreasing the system radius facilitates higher viable cell densities. Increasing the $pO_{2,in}$ from 70 to 90 mmHg results in larger regions of hypoxia and hyperoxia even at optimized cell densities. Increasing the PolyhHb concentration leads to curves with reduced hypoxia/hyperoxia at higher cell densities. This implies that using higher PolyhHb concentrations is one strategy for increasing the maximum viable cell density in a preexisting bioreactor.

The relationship between the theoretical Damköhler number and the combined hypoxic and hyperoxic fraction is shown in Figure 8. For the three $pO_{2,in}$ values, the trends observed are the same. Theoretical Damköhler values at the extrema led to low zonation. A theoretical Damköhler value between 1 and 8 minimizes the combined hypoxic and hyperoxic fraction. Theoretical Damköhler values outside this range lead to nonviable reactor configurations. This suggests that

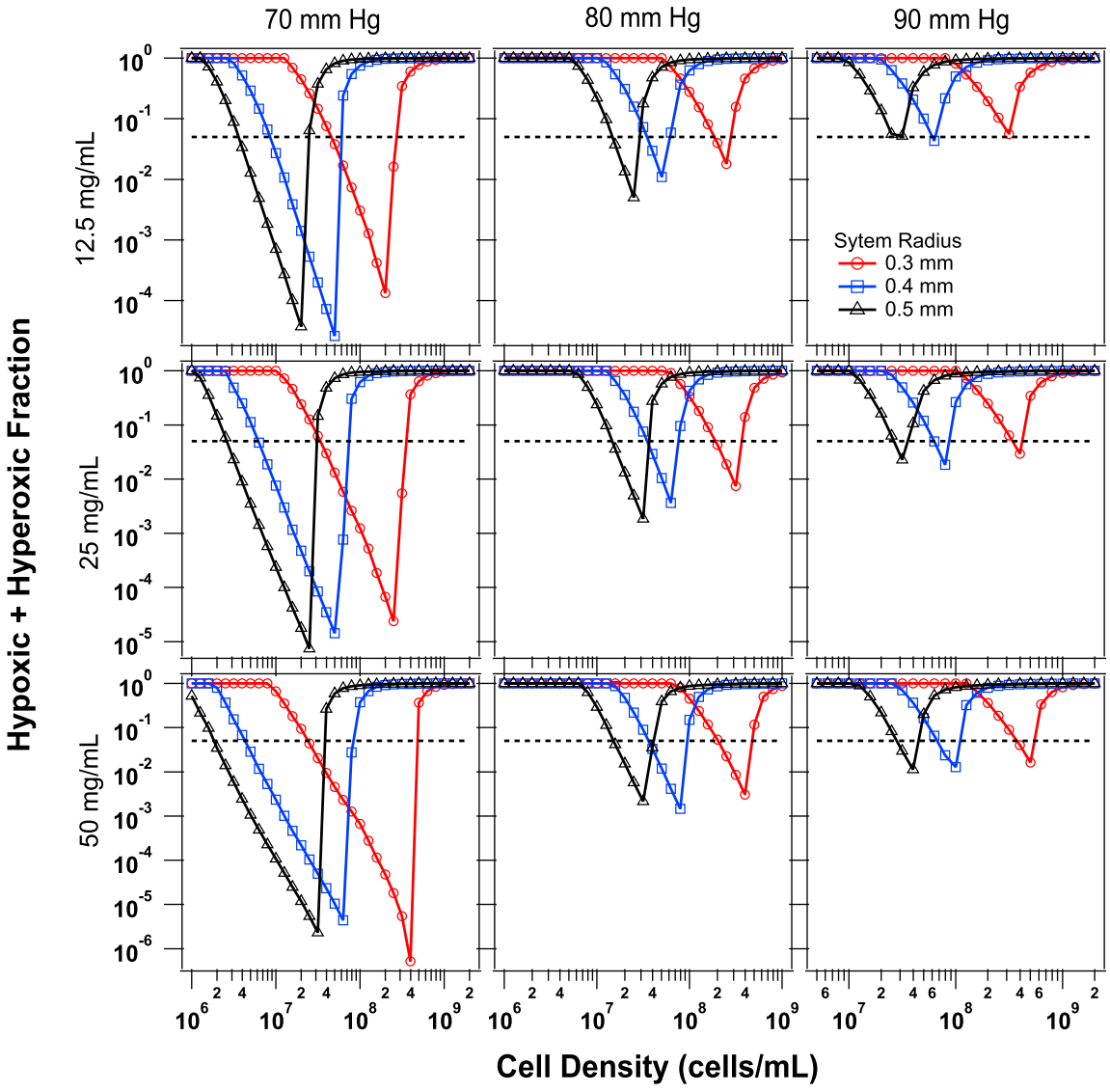

FIGURE 7 Hypoxic and hyperoxic fractions as a function of cell density for various bioreactor configurations and operating conditions. These figures show the hypoxic and hyperoxic fraction for media supplemented with T-state PolyhHb. The average concentration of PolyhHb in the media was varied from 12.5 to 50 mg/ml (rows), the $pO_{2,in}$ was varied from 70 to 90 mmHg (columns), and the radius of the system was varied from 0.3 to 0.5 mm. For these systems, the fiber length was 17 cm and the flow rate was 0.09 ml/min

if the theoretical Damköhler number can be calculated, it has the potential to strongly predict bioreactor performance. Due to the difficulty in its measurement, further analyses will be performed using the practical Damköhler number, which can be easily measured during bioreactor operation.

The relationship between the practical Damköhler and Sherwood number at three different $pO_{2,in}$ values and PolyhHb concentration of 12.5 mg/ml is shown in Figure 9. Shaded points correspond to viable bioreactor configurations with a combined hypoxic and hyperoxic volume fraction of less than 0.05. Increasing cell density is correlated with a higher Sherwood number. The Sherwood number itself appears to have little effect on the performance of the bioreactor since both low and high Sherwood values can lead to viable bioreactor conditions. By contrast, low and high practical Damköhler numbers tend to perform poorly. These trends hold at all inlet partial pressure conditions. Overall, the practical Damköhler number may also be predictive of the viability of the bioreactor.

The effect of the practical Damköhler number on the combined hypoxic and hyperoxic fraction is evident in Figure 10. Practical Damköhler numbers between 0.5 and 8 are necessary but not sufficient to minimize the combined fraction. Very low practical Damköhler numbers tend to lead to nonviable reactors with poor zonation. Very high practical Damköhler numbers also lead to nonviable reactors but generally offer improved zonation. This suggests that targeting a specific practical Damköhler number range may be beneficial in minimizing hypoxia and hyperoxia.

In comparison to the theoretical Damköhler number analyzed in Figure 8, the practical value follows a similar but not identical trend. The primary difference is that operating within the optimum range of the theoretical Damköhler number provides a higher probability of

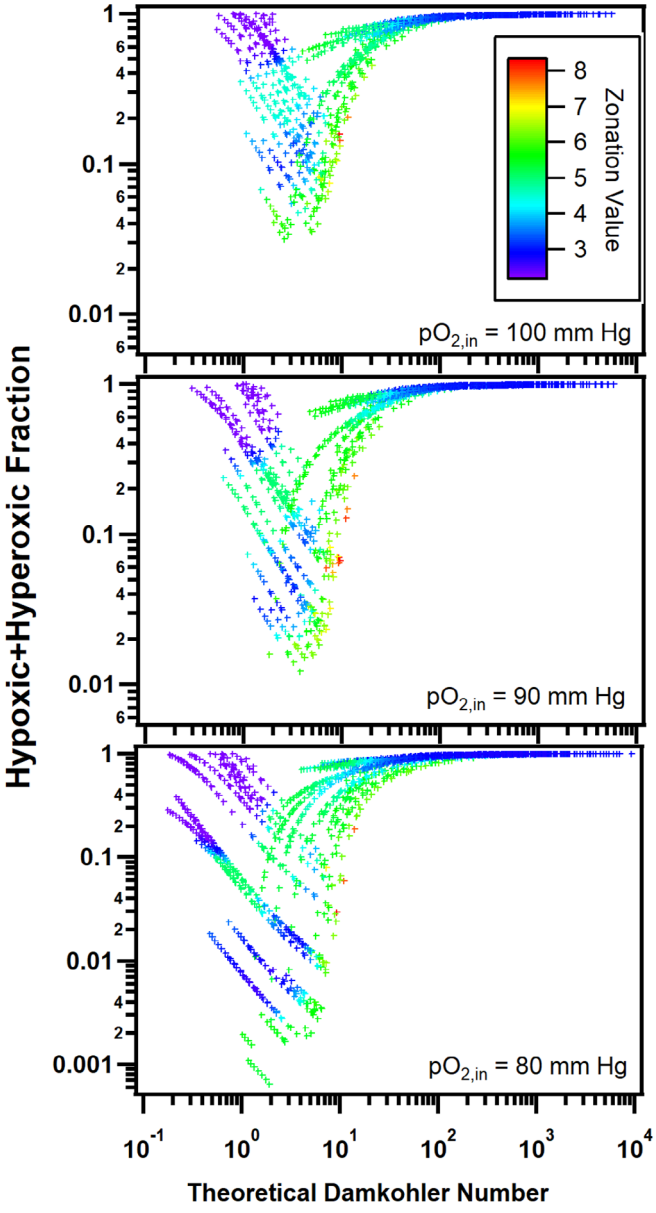

FIGURE 8 Hypoxic and hyperoxic fraction versus theoretical Damköhler number at (a) 80 mmHg, (b) 90 mmHg, and (c) 100 mmHg for a bioreactor supplemented with T-state PolyhHb. The PolyhHb concentration was 12.5 mg/ml with system radius, fiber length, flow rate, and cell density varying from 0.3–0.7 mm, 0.03–0.9 m, 0.05–0.7 ml/min, and 1×10^7–1×10^9 cells/ml, respectively

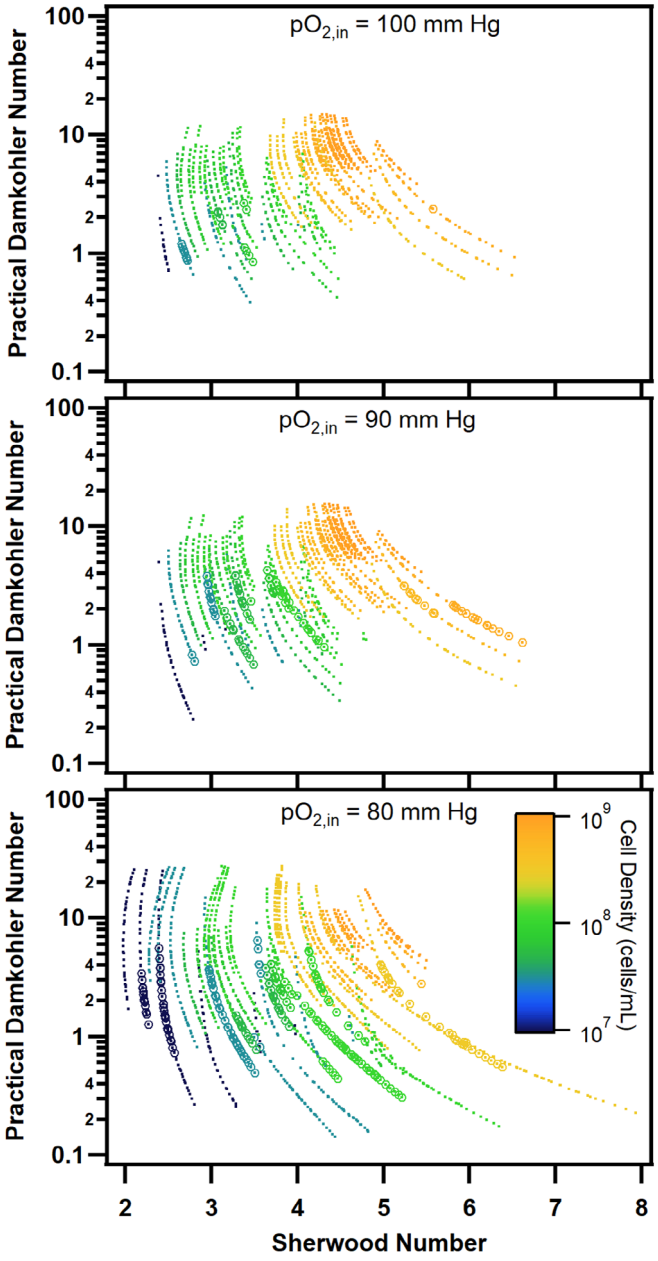

FIGURE 9 Practical Damköhler number versus Sherwood number at (a) 80 mmHg, (b) 90 mmHg, and (c) 100 mmHg for a bioreactor supplemented with T-state PolyhHb. The PolyhHb concentration was 12.5 mg/ml with system radius, fiber length, flow rate, and cell density varying from 0.3–0.7 mm, 0.03–0.9 m, 0.05–0.7 ml/min, and 1×10^7–1×10^9 cells/ml, respectively. Values with hypoxic/hyperoxic fractions less than 5% of the total volume are circled

producing a viable bioreactor configuration. The practical Damköhler number is not as predictive of zonation score with the optimum range still potentially leading to bioreactor configurations with large amounts of hypoxia and hyperoxia.

The effect of the Damköhler number on the zonation score when the data are filtered for viable bioreactor configurations is displayed in Figure 10. At 80 and 90 mmHg, higher zonation occurs at the upper edge of the viable range. The data at 100 mmHg are limited but shows that significant zonation is possible at lower Damköhler numbers as well. This suggests a very narrow margin of error when seeking to maximize zonation while maintaining bioreactor viability.

The correlation between the zonation score and the volume fraction of each zone in the bioreactor ECS is shown in Figure 11. All points correspond to viable bioreactor configurations with a combined hypoxic and hyperoxic fraction of less than 0.05. Low zonation scores are primarily characterized by the presence of two zones with one dominating the other. The three remaining zones are usually present in negligible amounts. A zonation score of 4.5 is the point at which a third zone appears and a zonation score of 5 signifies the point at which all three zones occupy nontrivial volume fractions of the ECS.

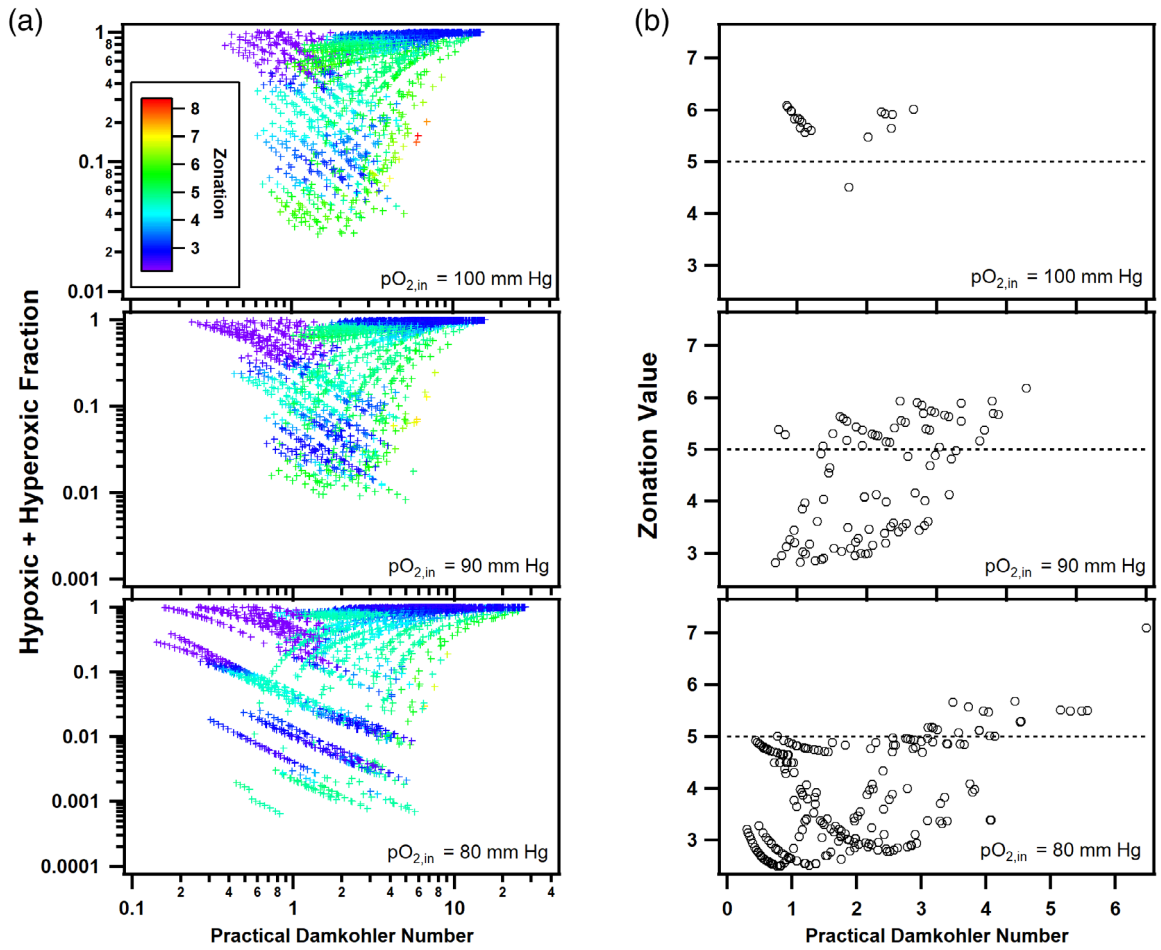

FIGURE 10 Effect of the practical Damköhler number on the (a) hypoxic + hyperoxic fraction and (b) zonation for a bioreactor supplemented with T-state PolyhHb. For each plot inlet, partial pressures of 100 mmHg (top), 90 mmHg (middle), and 80 mmHg (bottom) are shown. The PolyhHb concentration was 12.5 mg/ml with system radius, fiber length, flow rate, and cell density varying from 0.3–0.7 mm, 0.03–0.9 m, 0.05–0.7 ml/min, and 1×10^7 – 1×10^9 cells/ml, respectively

Above this point, two of the three zones start approaching parity with each other while the third zone remains as a relatively smaller region. Therefore, a zonation score of 5 can be regarded as a reasonable threshold for optimal zonation.

The false discovery rate (FDR) Log Worth plot of the combined hypoxic and hyperoxic volume fraction is shown in Figure 12a. All parameters have at least minor effects with cell density and system radius having the largest impact. The fiber length and flow rate have similar effects with $pO_{2,in}$ and PolyhHb concentration being close as well.

The FDR Log Worth plot of the Sherwood number is shown in Figure 12b. The system radius and cell density have the strongest correlation while $pO_{2,in}$ and the PolyhHb concentration have the lowest effect. The fiber length and flow rate have similar effects in the middle.

The FDR Log Worth plot of the Damköhler number is shown in Figure 12c. Here, the fiber length and flow rate have the strongest correlation while $pO_{2,in}$ has the lowest effect. The system radius, PolyhHb concentration, and cell density have relatively similar impacts.

The FDR Log Worth plot of the zonation score is displayed in Figure 12d. The cell density and $pO_{2,in}$ have the largest effects while

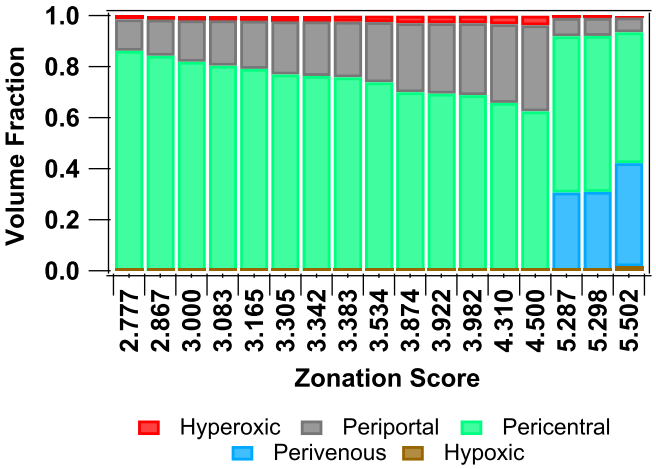

FIGURE 11 Category plot of volume fraction and zonation for a bioreactor supplemented with T-state PolyhHb. The PolyhHb concentration was 12.5 mg/ml while system radius, $pO_{2,in}$, and cell density were fixed at 0.62 mm, 80 mmHg, and 1×10^7 cells/ml, respectively. Fiber length and flow rate varied between 0.1–0.2 m and 0.03–0.3 ml/min

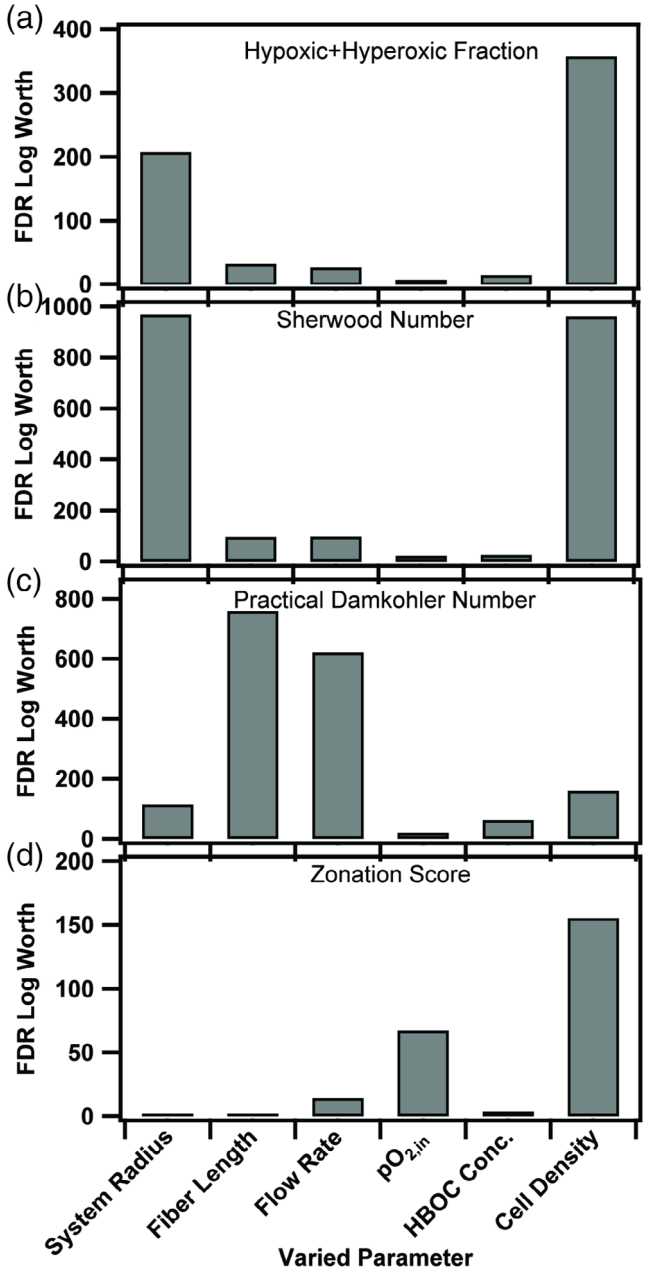

FIGURE 12 FDR Log Worth of (a) hypoxic + hyperoxic fraction, (b) Sherwood number, (c) Practical Damköhler number, and (d) zonation score. The average concentration of PolyhHb in the media was varied from 12.5 to 50 mg/ml (rows), the $pO_{2,in}$ was varied from 80 to 100 mmHg, the radius of the system was varied from 0.3 to 0.8 mm. The fiber length was varied from 3 to 90 cm, the flow rate was varied from 0.03 to 0.7 ml/min, and the cell density was varied from 1×10^7 to 1×10^9 cells/ml

PolyhHb concentration and flow rate have similar, smaller impacts. The system radius and fiber length both have the lowest correlation with zonation.

Overall, the cell density consistently had a fairly large impact on the four quantities while $pO_{2,in}$ and the PolyhHb concentration generally had smaller effects.

4 | CONCLUSIONS

Previous HBOCs failed to pass clinical trials due to safety complications attributed to significant amounts of low MW Hb species in solution. The PolyhHb synthesized in this study was purified to minimize the concentration of low MW Hb species in the final product, improving the safety of these materials for use in bioreactor circuits. Furthermore, the rate of auto-oxidation over a 24 hr time period was found to decrease after chemical cross-linking. This advancement will allow 30:1 T-state PolyhHbs to retain a large portion of their O_2 carrying capacity during bioreactor perfusion and enhance O_2 transport. Additionally, a program was designed to determine the polymeric composition of PolyhHbs and determine the size of various fractions. Using this program, we can verify the minimal presence of low MW Hb species, while simultaneously calculating the MW distribution of PolyhHb.

This study also shows that zonation in a bioreactor can be reasonably quantified via computational modeling. Furthermore, the Damköhler number may predict zonation as well as hypoxic and hyperoxic performance in a hepatic HF bioreactor. This may potentially aid in the optimal design and operation of such a bioreactor. Additional experimental work is needed to validate these computational findings and determine their application to real-world systems.

ACKNOWLEDGMENTS

We acknowledge Dr. James Lee (Chemical and Biomolecular Engineering, The Ohio State University) for allowing the use of his dynamic light scattering (DLS) spectrometer, and Marni Grevenow (Transfusion Services, Wexner Medical Center, The Ohio State University) for generously donating expired human RBC units. This work was supported by The Department of Defense Grant W81XWH-18-1-0059 as well as National Institutes of Health Grants R01HL126945, R01HL138116, and R01EB021926.

ORCID

Clayton Cuddington https://orcid.org/0000-0001-8739-2155
Donald Belcher https://orcid.org/0000-0002-7633-6219
Niral Ramesh https://orcid.org/0000-0001-9649-1665

REFERENCES

1. Eghbali H, Nava MM, Mohebbi-Kalhori D, Raimondi MT. Hollow fiber bioreactor technology for tissue engineering applications. *Int J Artif Organs*. 2016;39:1-15.
2. Hirschel M, Gangemi JD, McSharry J, Myers C. Novel uses for hollow fiber bioreactors. *Genet Eng Biotechnol News*. 2011;31:42-44.
3. Gordon J, Dare MR, Palmer AF. Engineering select physical properties of cross-linked red blood cells and a simple a priori estimation of their efficacy as an oxygen delivery vehicle within the context of a hepatic hollow fiber bioreactor. *Biotechnol Prog*. 2005;21:1700.
4. Chen G, Palmer AF. Hemoglobin-based oxygen carrier and convection enhanced oxygen transport in a hollow fiber bioreactor. *Biotechnol Bioeng*. 2009;102:1603-1612.
5. Jones JA. Red blood cell substitutes: current status. *Br J Anaesth*. 1995;74:697-703.

6. Rifkind JM, Ramasamy S, Manoharan PT, Nagababu E, Mohanty JG. Redox reactions of hemoglobin. *Antioxid Redox Signaling*. 2004;6:657-666.
7. Alayash AI, D'Agnillo F, Buehler PW. First-generation blood substitutes: what have we learned? Biochemical and physiological perspectives. *Expert Opin Biol Ther*. 2007;7:665-675.
8. Kim HW, Greenburg AG. Artificial oxygen carriers as red blood cell substitutes: a selected review and current status. *Artif Organs*. 2004; 28:813-828.
9. Alayash AI. Hemoglobin-based blood substitutes and the treatment of sickle cell disease: more harm than help? *Biomolecules*. 2017;7:16-28.
10. Moradi S, Jahanian-Najafabadi A, Roudkenar MH. Artificial blood substitutes: first steps on the long route to clinical utility. *Clin Med Insights: Blood Disord*. 2016;9:33-41.
11. Silverman TA, Weiskopf R. Hemoglobin-based oxygen carriers session I: setting the stage. *Anesthesiology*. 2009;111:946-963.
12. Habeeb AF, Hiramoto R. Reaction of proteins with glutaraldehyde. *Arch Biochem Biophys*. 1968;126:16-26.
13. Butt OI, Buehler PW, D'Agnillo F. Differential induction of renal heme oxygenase and ferritin in ascorbate and nonascorbate producing species transfused with modified cell-free hemoglobin. *Antioxid Redox Signaling*. 2010;12:199-208.
14. Butt OI, Buehler PW, D'Agnillo F. Blood-brain barrier disruption and oxidative stress in Guinea pig after systemic exposure to modified cell-free hemoglobin. *Am J Pathol*. 2011;178:1316-1328.
15. Tsai AG, Cabrales P, Manjula BN, Acharya SA, Winslow RM, Intaglietta M. Dissociation of local nitric oxide concentration and vasoconstriction in the presence of cell-free hemoglobin oxygen carriers. *Blood*. 2006;108:3603-3610.
16. Cabrales P, Tsai AG, Intaglietta M. Polymerized bovine hemoglobin can improve small-volume resuscitation from hemorrhagic shock in hamsters. *Shock*. 2009;31:300-307.
17. Belcher DA, Banerjee U, Baehr CM, et al. Mixtures of tense and relaxed state polymerized human hemoglobin regulate oxygen affinity and tissue construct oxygenation. *PLoS One*. 2017;12:1-22.
18. Buehler PW, Zhou Y, Cabrales P, et al. Synthesis, biophysical properties and pharmacokinetics of ultrahigh molecular weight tense and relaxed state polymerized bovine hemoglobins. *Biomaterials*. 2010;31: 3723-3735.
19. Elmer J, Harris DR, Sun G, Palmer AF. Purification of hemoglobin by tangential flow filtration with diafiltration. *Biotechnol Prog*. 2009;25: 1402-1410.
20. Mareels G, Poyck PP, Eloot S, Chamuleau RA, Verdonck PR. Three-dimensional numerical modeling and computational fluid dynamics simulations to analyze and improve oxygen availability in the AMC bioartificial liver. *Ann Biomed Eng*. 2006;34:1729-1744.
21. De Bartolo L, Salerno S, Curcio E, et al. Human hepatocyte functions in a crossed hollow fiber membrane bioreactor. *Biomaterials*. 2009;30: 2531-2543.
22. Kietzmann T. Metabolic zonation of the liver: the oxygen gradient revisited. *Redox Biol*. 2017;11:622-630.
23. Palmer AF, Sun G, Harris DR. Tangential flow filtration of hemoglobin. *Biotechnol Prog*. 2009;25:189-199.
24. Palmer AF, Sun G, Harris DR. The quaternary structure of tetrameric hemoglobin regulates the oxygen affinity of polymerized hemoglobin. *Biotechnol Prog*. 2009;25:1803-1809.
25. Zhang N, Jia Y, Chen G, Cabrales P, Palmer AF. Biophysical properties and oxygenation potential of high-molecular-weight glutaraldehyde-polymerized human hemoglobins maintained in the tense and relaxed quaternary states. *Tissue Eng Part A*. 2011;17:927-940.
26. Winterbourn CC. Oxidative reactions of hemoglobin. *Methods Enzymol*. 1990;186:265-272.
27. Arifin DR, Palmer AF. Determination of size distribution and encapsulation efficiency of liposome-encapsulated hemoglobin blood substitutes using asymmetric flow field-flow fractionation coupled with multi-angle static light scattering. *Biotechnol Prog*. 2003;19:1798-1811.
28. Hill AV. Proceedings supplement: the possible effects of the aggregation of the molecules of haemoglobin on its dissociation curves. *J Physiol*. 1910;40:iv-vii.
29. Jahr JS, MacKenzie C, Pearce LB, Pitman A, Greenburg AG. HBOC-201 as an alternative to blood transfusion: efficacy and safety evaluation in a multicenter phase III trial in elective orthopedic surgery. *J Trauma Inj Infect Crit Care*. 2008;64:1484-1497.
30. LaMuraglia GM, O'Hara PJ, Baker WH, et al. The reduction of the allogenic transfusion requirement in aortic surgery with a hemoglobin-based solution. *J Vasc Surg*. 2000;31:299-308.
31. Napolitano LM. Hemoglobin-based oxygen carriers: first, second or third generation? human or bovine? Where are we now? *Crit Care Clin*. 2009;25:279-301.
32. Lou Carmichael FJ, Ali AC, Campbell JA, et al. A phase I study of oxidized raffinose cross-linked human hemoglobin. *Crit Care Med*. 2000; 28:2283-2292.
33. Faivre B, Menu P, Labrude P, Vigneron C. Hemoglobin autooxidation/oxidation mechanisms and methemoglobin prevention or reduction processes in the bloodstream: literature review and outline of autooxidation reaction. *Artif Cells Blood Substit Immobil Biotechnol*. 1998;26:17-26.
34. Xu H, Bjerneld EJ, Käll M, Börjesson L. Spectroscopy of single hemoglobin molecules by surface enhanced Raman scattering. *Phys Rev Lett*. 1999;83:4357-4360.
35. Gozzelino R, Jeney V, Soares MP. Mechanisms of cell protection by heme oxygenase-1. *Annu Rev Pharmacol Toxicol*. 2010;50:323-354.
36. Laskowski RA, Gerick F, Thornton JM. The structural basis of allosteric regulation in proteins. *FEBS Lett*. 2009;583:1692-1698.
37. Palmer AF, Zhang N, Zhou Y, Harris DR, Cabrales P. Small-volume resuscitation from hemorrhagic shock using high-molecular-weight tense-state polymerized hemoglobins. *J Trauma Inj Infect Crit Care*. 2011;71:798-807.
38. Day TK. Current development and use of hemoglobin-based oxygen-carrying (HBOC) solutions. *J Vet Emerg Crit Care*. 2003;13:77-93.
39. Larsen R, Gozzelino R, Jeney V, et al. A central role for free heme in the pathogenesis of severe sepsis. *Sci Transl Med*. 2010;2:1-12.
40. Smith A, McCulloh RJ. Hemopexin and haptoglobin: allies against heme toxicity from hemoglobin not contenders. *Front Physiol*. 2015; 6: 148.
41. Tsuruga M, Matsuoka A, Hachimori A, Sugawara Y, Shikama K. The molecular mechanism of autoxidation for human oxyhemoglobin. Tilting of the distal histidine causes nonequivalent oxidation in the β chain. *J Biol Chem*. 1998;273:8607-8615.
42. Jia Y, Wood F, Menu P, Faivre B, Caron A, Alayash AI. Oxygen binding and oxidation reactions of human hemoglobin conjugated to carboxylate dextran. *Biochim Biophys Acta - Gen Subj*. 2004;1672:164-173.
43. Meng F, Kassa T, Jana S, et al. Comprehensive biochemical and biophysical characterization of hemoglobin-based oxygen carrier therapeutics: all HBOCs are not created equally. *Bioconjug Chem*. 2018;29:1560-1575.
44. Buehler PW, Boykins RA, Jia Y, Norris S, Freedberg DI, Alayash AI. Structural and functional characterization of glutaraldehyde-polymerized bovine hemoglobin and its isolated fractions. *Anal Chem*. 2005;77:3466-3478.
45. Ali AA, Ali GS, Steinke JM, Shepherd AP. Co-oximetry interference by hemoglobin-based blood substitutes. *Anesth Analg*. 2001;92:863-869.

How to cite this article: Cuddington C, Moses S, Belcher D, Ramesh N, Palmer A. Next-generation polymerized human hemoglobins in hepatic bioreactor simulations. *Biotechnol Progress*. 2020;36:e2958. https://doi.org/10.1002/btpr.2958